Flow swirl and flow profile measurement in multiphase flow

Anusha Rammohan[1], *Aditya Bhakta*[1], *Vinay Natrajan*[1], *John Ward*[2], and *Manoj Kumar KM*[1]

[1]GE Global Research, Bangalore, India
[2]GE Oil and Gas - Measurement and Control, Groby, UK

Abstract

Accurate multiphase flow measurement hinges on the ability to measure flow parameters such as component phase fractions and velocities with high accuracy. Since, the fractions and velocities are not always uniformly distributed in the measurement cross section, any measurement system's inability to account for spatial variations can result in a high degree of uncertainty in the estimated flow rate. This paper describes a method using an impedance based measurement system using which the profiles of phase fraction and velocity for a vertical pipe downstream of a blind tee can be measured and characterized. Using the same measurement, a modified cross correlation technique provides the vertical and horizontal components of the velocity in a swirling flow. This velocity information along with the phase fraction profile characterizes the flow profile completely. In addition to this analysis, the potential effect of swirl on differential pressure measurements is addressed briefly.

Nomenclature

τ_{max}^{ij}	Time shift corresponding to maximum cross correlation for pixel ij, page 6
P	Pressure, page 13
$R_{xy}^{ij,kl}$	Cross correlation of series x at pixel ij with y at pixel kl, page 10
R_{xy}^{ij}	Cross correlation of series x and y at pixel ij, page 6
V_{ij}	Velocity measured at pixel ij, page 6
ρ	Density, page 12

τ Time shift for cross correlation, page 6

dP Differential pressure, page 12

d_{rad}^{ij} Radial distance traveled by pixel ij, page 10

d_{ax} Axial distance between cross correlation planes, page 10

r, θ, z Cylindrical coordinates, page 12

t Time instant, page 6

t Time instant, page 12

u_r Radial component of velocity, page 12

u_θ Angular component of velocity, page 12

u_z Vertical/Axial component of velocity, page 12

x_{ij},y_{ij} Time series at two planes of measurement at pixel ij, page 6

GVF Gas volume fraction, page 4

WLR Water in liquid ratio, page 4

1 Introduction

One of the biggest challenges in multiphase flow metering is the presence of varying spatial distributions of the different fluids within the cross section of the pipe. Any measurement technique employed in a multiphase flow meter is expected to measure the flow parameters of interest with the same fidelity irrespective of the cross sectional distribution including asymmetries and non-uniformities in the flow profile. This requirement is extended to the velocities as well as component fractions. Additionally, the implicit but ubiquitous assumption in most flow rate measurement systems is that the fluid flow is always parallel to the pipe. For example, for vertically placed flowmeters, the flow is assumed to be restricted to the vertical direction. These assumptions and approximations can result in significant inaccuracy when the flow is asymmetric or irregular.

Most multiphase measurement methods tackle this problem in one of two ways. One approach is to condition the flow with some sort of a flow conditioner to ensure flow profiles that are favourable for measurement. A popular configuration is to use a blind tee with the meter placed in the vertical section of the flow. But the effectiveness of flow conditioners such as the blind tee has not been proven conclusively under all flow conditions. For instance the blind tee can cause gas holdup or induce swirl. The only alternative is to correct for the existence of non-uniform flow profiles. This in turn requires two pieces of information, a) the actual flow profiles and flow direction at the measurement section and b) a translation of the flow profile into a suitable measurement model. Generally speaking, accurate flow profiles are difficult to measure. This is especially the case for sensor measurements that do not cover the entire cross section or are unable to resolve radial or even temporal variations. Given this potential lack of information, the measurement models have to be tweaked using empirical calibration instead of measured flow profiles in the hope of capturing the missing information. As with any data based technique, the performance of the corrected models can become inaccurate at best and unpredictable at worst.

An important step towards understanding the impact of the errors due to flow profile and flow direction variation on multiphase measurement is to first characterize it. This paper proposes a method to measure and characterize the flow by quantifying the variation of velocity (magnitude and direction) and component fractions in the flow cross section. For the purpose of this paper, we have considered vertical three phase flows consisting of gas, water and oil. The measurement system consisted of two sets of electrical impedance sensors placed axially separated in the vertical section downstream of a blind tee. Section 2 describes the process of flow profile measurement and characterization. Section 3 describes the detailed analysis of the phase fraction and velocity profiles measured with the proposed method under different flow conditions for two different configurations. Section 4 focuses specifically on measuring and quantifying flow swirl and

how errors due to swirl can be corrected. Section 5 concludes this paper with a summary of the key learning from this work and possible opportunities for future studies.

2 Flow profile measurement

Accurate multiphase flow measurement, invariably needs flow physics or semi-empirical models in conjunction with suitable measurement technologies for estimating the fractions and velocities of individual components. A detailed description of these models are provided in Rammohan et al. [9]. While typical flow models are well grounded in physics, certain approximations are made either because they make the analysis easier or because the necessary information is missing or hard to determine. One such assumption is about symmetry and uniformity of flow profiles. Apart from flow models, several sensor measurement models also make the same assumption. Ideally, the flow is expected to be uniform and time-invariant but that is rarely the case especially under real field conditions. Not only does the flow change over space and time, the changes are rather hard to predict even if the flow conditions are completely known. While empirical models can be built with historical data to predict non-uniformities or correct for them, there is no guarantee that these corrections will work under conditions outside the limits of the historical data. Thus, the only way to accurately and reliable correct for profile non-uniformities in the model, is to measure the actual flow profile using a suitable measurement technique.

Earlier attempts have been made to measure the phase fraction and velocity profiles using tomographic techniques (Abdulkadir et al. [1], Ohnuki and Akimoto [8], Thiyagarajan et al. [10]). Researchers have also quantified the shape of the measured flow profiles for different flow conditions, which can then be readily used in flow models. Detailed though these studies are, there are several key pieces of information missing:

- ✗ Flow profiles are mostly defined and characterized for fully developed flow. There is little information on profiles in developing multiphase flows (downstream of a blind tee in specific).
- ✗ Potential asymmetries in the flow have been explored for inclined pipes (where asymmetries are expected to occur) but not for vertical flows. (Al-Hinai [2])
- ✗ Flow irregularities such as flow swirl have not been measured or characterized for multiphase flow.

In this paper, we hope to address these important aspects with the aid of a suitable measurement technique followed by a detailed analysis of the measurement data.

2.1 Impedance measurement system and experimental setup

Electrical sensors have been widely used for measurement of phase distributions in multiphase flows. This is mainly due to the accuracy of the measurement and ease of interpretation of the data. Moreover, using a multitude of impedance sensors, the cross sectional distribution of the dispersed phase can be reconstructed with higher resolution and accuracy. The details of a preferred reconstruction method are disclosed in Mahalingam et al. [6] and Mahalingam et al. [5]. This method is fast, less computationally complex than traditional reconstruction, robust and accurate in reconstructing the spatial distribution of the dispersed phase, which in this case is the gas phase. The measurement system consists of 2 sets of electrodes along the circumference of the pipe placed spatially apart in the direction of the flow. A high speed data acquisition and data processing system provides reconstructed fraction phase images at around 2000 frames/s. This configuration with the capability for high speed acquisition is conducive for not only capturing instantaneous changes in the flow cross section, but also for velocity measurement with high resolution. The subsequent sections describe detailed analysis using the measurements from the same impedance measurement system but placed with different pipe configurations, at different distances from the blind tee and with test data collected at different loops including the National Engineering Lab (NEL) in Scotland, UK and the South West Research Institute(SWRI) at Texas, USA. The configuration and test setup for the data presented in this paper are listed in Table 1.

Test site	**NEL**	**SWRI**
Measurement distance from blind tee	35D	5D
GVF range	0-95%	0-95%
WLR range	0-100%	0-100%
Liquid flow rate	15000 bbl/day	26000 bbl/day
Gas flow rate	1.3 acfs	1.7 acfs
Pressure	5 bar	10-100 bar
Horizontal run to blind tee	35 m	1 m

Table 1: Test conditions

All data for the test points presented in this paper are averaged over 2 minutes, after it was ensured that the reference readings were stabilized. It is important to note here that the stability established in this manner is indicative of the inlet conditions only. Once, the flow is mixed, it is hard to guarantee stability at the measurement location.

2.2 Phase fraction and velocity profile measurement

Typical flow profiles as reconstructed using the impedance measurements are shown in figures 1a and 1b at two different gas volume fractions. Each pixel in the image is an average phase fraction for the area covered by that pixel. The best possible pixel resolution is related to pipe diameter and the number of impedance sensors placed on the circumference of the pipe.

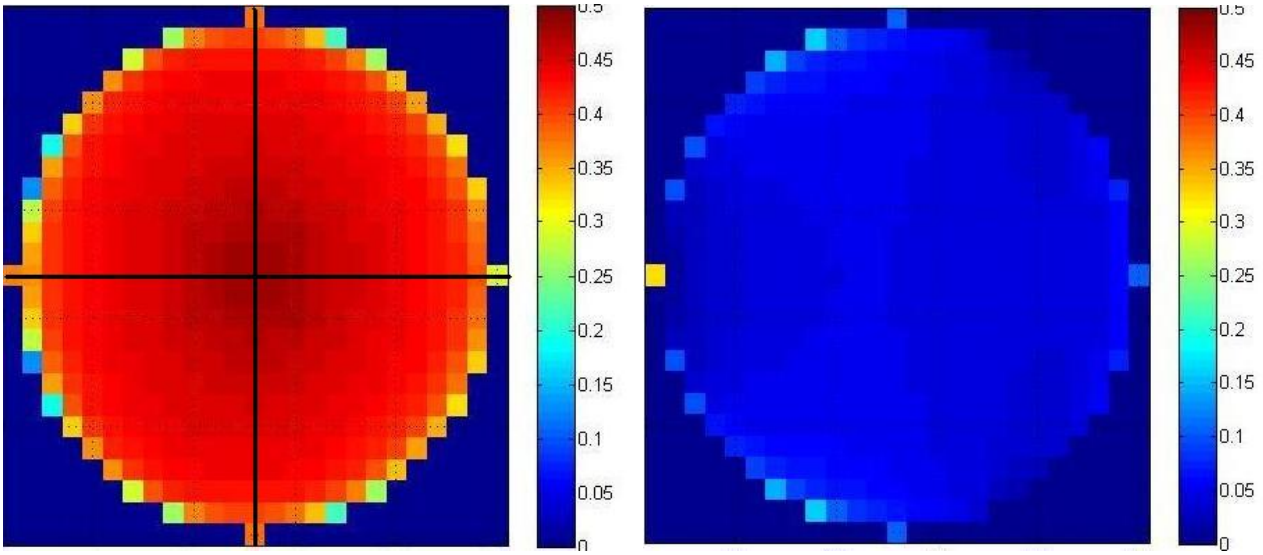

(a) GVF=50% (b) GVF=20%

Figure 1: *Phase fraction profiles in the pipe cross section reconstructed from impedance measurements (NEL test data)*

As is evident from these figures, the cross sectional phase fraction profile thus generated provide valuable information about the distribution of the gas and in turn the liquid as well. A more detailed analysis of phase fraction profiles under different flow conditions is covered in section 3.

With the measurements from two spatially separated sets of impedance sensors, there is the added possibility of obtaining the flow velocity using cross correlation of the images. Image cross correlation is a recently explored technique for estimating the distribution of velocity within the cross section. A straight forward implementation of the image cross correlation technique involves the following steps:

1. For a particular pixel in the i^{th} column and j^{th} row in the image, create time series in plane 1 and 2 from the reconstructed phase fraction

2. Cross correlate the two time series using the expression

$$R_{xy}^{ij}(\tau) = \sum_{t=0}^{N} x_{ij}(t) y_{ij}(t-\tau) \tag{1}$$

3. From the time shift τ for which the cross correlation is maximum, find the velocity at location ij, given the distance between the sensors using

$$V_{ij} = d_{ax}/\tau_{max}^{ij} \tag{2}$$

4. Repeat steps 1-3 for all pixels to obtain a *Velocity Map*

Figure 2 shows typical velocity maps obtained using the method described above. Section 3 explores the variation in the velocity profile under different conditions in more detail.

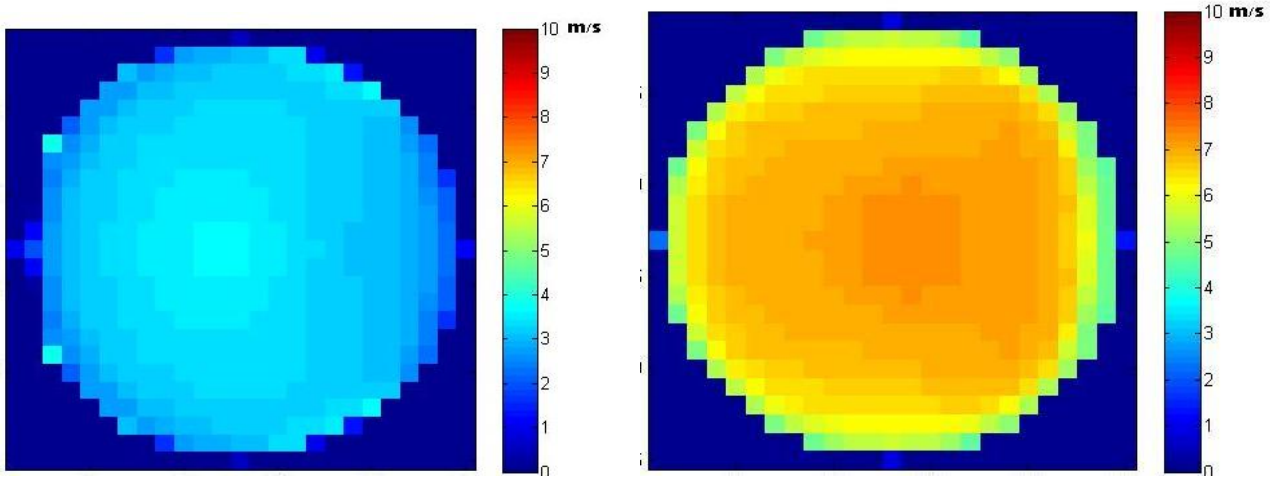

(a) Total superficial velocity = 2.7 m/s

(b) Total superficial velocity = 6.8 m/s

Figure 2: *Velocity maps using image cross correlation; color-map shows magnitude of velocity(NEL test data)*

3 Phase fraction and velocity profile analysis

3.1 Developed flow

Developed flow conditions are ideal for studying and characterizing the variations of phase fraction and velocity profiles for different flow rates. Hence, this topic has formed the theme for several prior work that

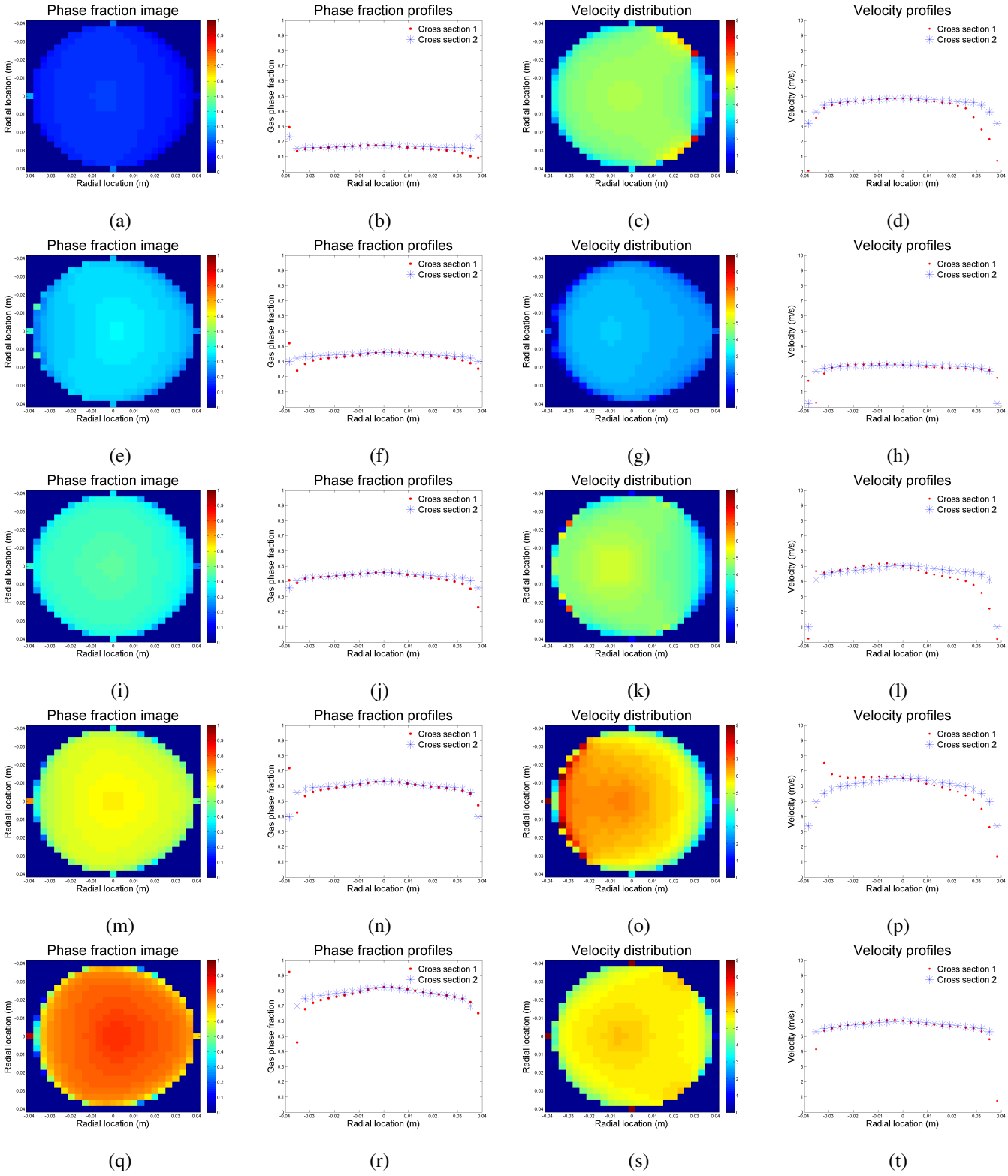

Figure 3: *Phase fraction and velocity profiles for developed flow (NEL data): (a) to (d) at 15% GVF, (e) to (h) at 30% GVF, (i) to (l) at 50% GVF, (m) to (p) at 70% GVF, (q) to (t) at 90% GVF*

involved characterizing and quantifying flow profiles (Abdulkadir et al. [1],Ohnuki and Akimoto [8],Thiyagarajan et al. [10]). A significant portion of published literature on this topic focused on smaller diameter pipes; the applicability of the conclusions needs to be considered carefully for larger diameters (say more than 4"). If there is a dearth of references on phase fraction profiles, there is even less work on velocity profiles in multiphase flow. This is due to the fact that unlike phase fraction distributions which can be obtained by several different types of sensors, the velocity distribution especially in a multiphase flow is generally not very easy to measure using simple sensors and/or data acquisition systems. Al-Hinai [2] analyzed both phase fraction and velocity distributions in vertical as well as inclined pipes using impedance based measurements but for solid-liquid flows.

The experimental data collected at NEL fits the category of developed flow as the distance from the blind tee to the measurement location was close to 35 times the diameter. Figure 3 shows the experimentally determined phase fraction and velocity profiles in the cross section for increasing GVF. For the profiles shown in figures 3a through 3t, the WLR was kept almost a constant at 80% in order to study the effect of gas and liquid flow rate variations. The first column of figures are images of phase fraction reconstructed from the impedance data. The second column shows two perpendicular radial cross sections (cross hairs indicated in figure 1a). The third column shows the corresponding velocity distributions obtained through cross correlation. The fourth column shows extracts of this distribution for two perpendicular radial cross sections.

Several interesting observations can be made from figure 3 for developed flow under the flow conditions tested at NEL.

- ☛ Phase fraction profiles are radially symmetric and well defined. They follow patterns described in literature for developed flow.
- ☛ At lower phase fractions (and lower GVF), the difference between the gas phase phase fraction near the wall and at the centre is not as pronounced in comparison with higher GVF flow conditions. This is consistent with the expectation that the flow transitions from bubbly to slug to churn and churn-annular and this transition is approximately related to increasing GVF.
- ☛ Velocity profiles are well defined but for certain flow conditions (pronounced at higher total flow rates) there is undeniable radially asymmetry in the distribution. This asymmetry is consistently seen only along one of the radial cross sections.
- ☛ All the flow conditions depicted in figure 3 are likely to be in the turbulent regime, a fact that is corroborated by the nearly flat velocity profiles for most of the conditions tested.

3.2 Developing flow

Mutliphase flow meters are rarely given the luxury of sufficient development length due to constraints on the piping and placement of the meter. Thus, from a practical point of view, meters are more likely to encounter under developed or developing flows. Developing flows are not the most most favourable conditions from a measurement perspective. Hence, a flow conditioner such as a blind tee is typically placed upstream of the meter in order to ensure mixing of the different phases. An ideally mixed flow has advantages for measurement as it allows for certain assumptions such as radial symmetry in flow profiles and minimal slip between the phases to name a few. But these assumptions are only valid if the blind tee does result in an ideally mixed flow. With the above described techniques for measurement of flow profiles, such assumptions on the flow profile can be easily investigated.

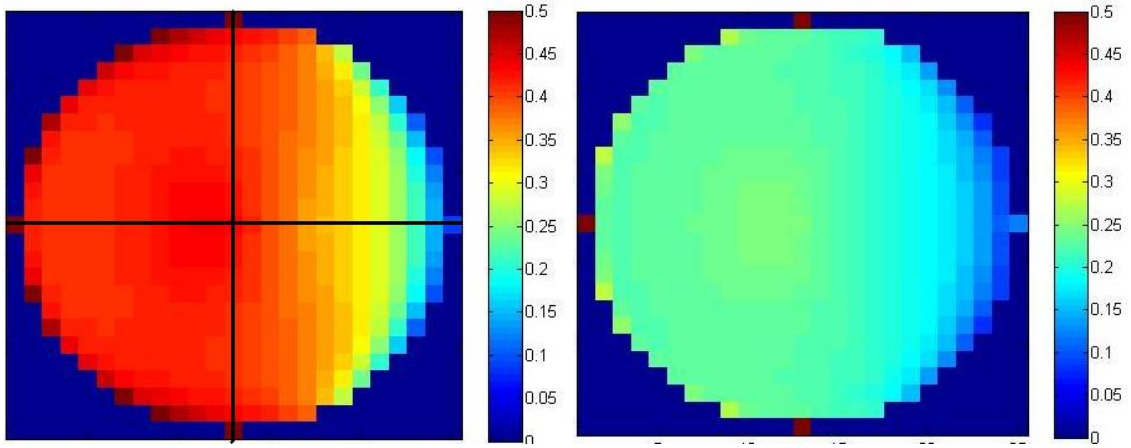

(a) GVF=40% (b) GVF=25%

Figure 4: *Phase fraction image from impedance measurements (SWRI test data, no development length)*

The data presented in this section have been acquired during a month long test at the South West Research Institute (SWRI) for varying flow conditions. For this particular analysis, a subset of the data was used where the WLR was again kept almost invariant at 80% and the line pressure was maintained at 100 bar in order to study the variation with flow rates.

The phase fraction images shown in figure 4 were obtained using the same method as the one used for the analysis of the NEL test data. Figures 4a and 4b clearly show radial asymmetry in the distribution of gas. To understand this asymmetry, one needs to understand the configuration of the measurement system with respect to the blind tee. Figure 5 shows the view of the reconstructed phase fraction image from the top (looking down the vertical section).

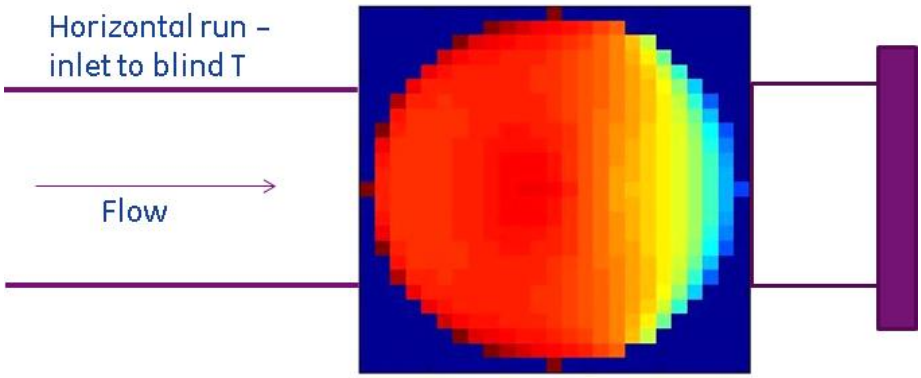

Figure 5: *Configuration of blind tee with respect to the reconstructed phase fraction image (view from top)*

Quite evidently, the asymmetry is in the direction of the inlet to the blind tee. This would make sense as the blind tee may not be the ideal mixer that it is touted to be. It is not hard to imagine a situation where there is stratified, plug or slug flow in the horizontal section before the blind tee with the gas being concentrated predominantly on the top part of the pipe above the liquid. If the blind tee doesn't mix the contents as is it expected to, then this flow would continue undisturbed onto the vertical section where the asymmetry would be apparent with the gas being more concentrated in the section on the same side as the inlet to the blind tee. This theory would then explain the radially asymmetry seen in the figure 4. 6 shows more such phase fraction distributions and profiles in the figures in columns 1 and 2. The profiles along the two selected radial cross sections show a pronounced asymmetry in stark contrast to the profiles from the NEL data (figure 3). Clearly the asymmetry is systemic and is seen for most of the flow conditions tested.

The third and fourth columns of figure 6 depict velocity profiles for varying GVF. There are small asymmetries for some of the data, but these seem insignificant, especially in comparison with the asymmetries in phase fraction. Also, in comparison with the velocity profiles for developed flow, (figure 3), the profiles in figure 6 for a location next to the blind tee are flatter and show little variation going from the center to the wall. This could quite easily be a characteristic of developing flows.

Even though the flow conditions tested at NEL and SWRi were different (Eg, fluids, ranges of flow rates, differences in loop configurations), two aspects of interest were the development length and the upstream horizontal run upto the blind tee. From the data presented here as well as that in literature, development length is quite likely to be a determining factor for the phase distribution within the cross section. But more importantly, with the kind of distributions seen in figure 6, mutliphase models cannot be justified in assuming radially symmetric profiles.

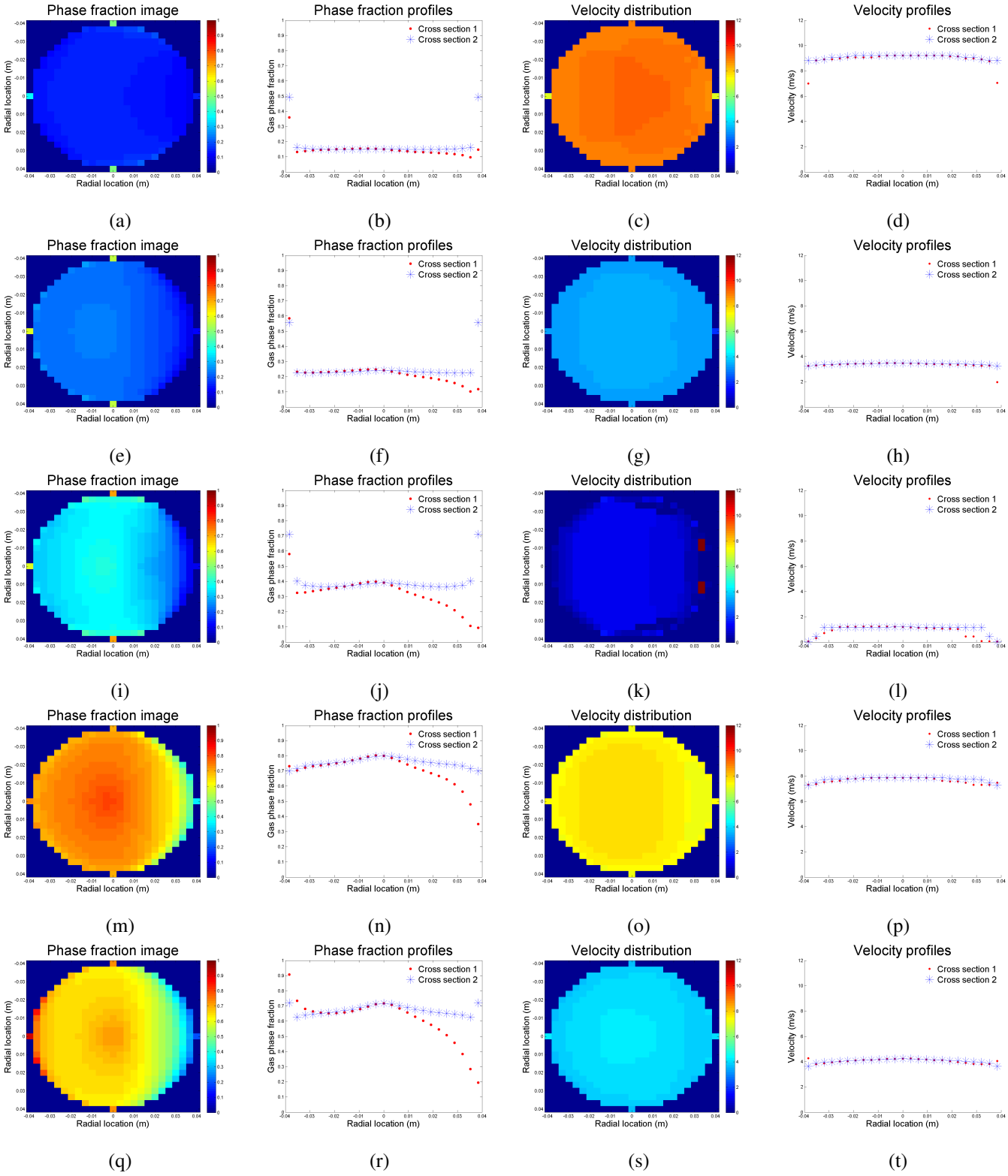

Figure 6: *Phase fraction and velocity profiles for developing flow (SWRI data): (a) to (d) at 15% GVF, (e) to (h) at 40% GVF, (i) to (l) at 50% GVF, (m) to (p) at 70% GVF, (q) to (t) at 80% GVF*

4 Flow swirl analysis

While the phase fraction distribution and velocity distributions provide a clearer picture of the evolution of the flow at the measurement location, flow characterization is incomplete without analyzing the direction of the velocity. Conventional wisdom dictates that a developed flow in a vertical pipe would flow only in the vertical direction with little deviations in the horizontal directions. This assumption would definitely ease the burden of flow measurement as it simplifies the problem to a great extent. But the existence of horizontal components to the velocity could potentially affect multiphase measurement systems including sensors such as the differential pressure sensors. Gibson and Reader-Harris [3] and Gupta and Kumar [4] analyzed swirl in single phase flow using both CFD simulations as well as measurements from particle image velocimetry techniques. Gibson and Reader-Harris [3] also looked at the effect of swirl on a venturi and an orifice plate placed downstream of a double bend and characterized the variation of the discharge coefficient with the swirl angle.

In this paper, we specifically focus on measuring swirl in mutliphase flow downstream of a blind tee. Furthermore, we demonstrate the potential effects of swirl on differential pressure measurements across a venturi.

4.1 Flow swirl measurements

By its very design, the image cross correlation method described in the section 2.2 estimates only the axial (vertical) component of the velocity and the drawback here is the assumption that the flow is parallel to the pipe. When the flow is not unidirectional and there may be swirling flows, this can be a limiting assumption that is likely to affect the accuracy of the velocity estimate. Moreover this method does not provide any information about other components of velocity, for example, the in-plane (in the plane of the measurement cross section) velocity component. If there existed a method that could measure a 3 dimensional velocity map, this would undoubtedly be a powerful piece of information for not just understanding the flow better, but also for augmenting simplistic flow models that assume unidirectional flow.

Mosorov et al. [7] described a method they called the "best-correlation pixels" to allow for particles traveling possibly at different angles with respect to the pipe. The algorithm is a modified version of the steps described in section 2.3 and proceeds as follows:

1. For a particular pixel in the i^{th} column and j^{th} row in the image, create time series in plane 1 and 2 from the reconstructed phase fraction

2. Cross correlate the two time series using the expression

$$R_{xy}^{ij}(\tau) = \sum_{t=0}^{N} x_{ij}(t) y_{ij}(t-\tau) \tag{3}$$

3. Repeat steps 1 and 2 with i and j changing for plane 2 such that it scans a region in the image around pixel ij using the following modified cross correlation

$$R_{xy}^{ij,kl}(\tau) = \sum_{t=0}^{N} x_{ij}(t) y_{kl}(t-\tau) \tag{4}$$

where $k \in [i-m, i+m]$ and $l \in [j-m, j+m]$

4. Find pixel l and k which maximizes $R_{xy}^{ij,kl}(\tau)$ and the corresponding time shift τ

5. From the time shift τ_{max} for which the cross correlation is maximum, find the axial velocity, given the distance between the sensors using

$$Vaxial_{ij} = d_{ax}/\tau_{max}^{ij} \tag{5}$$

The radial component of the velocity is given by

$$Vradial_{ij} = d_{rad}^{ij}/\tau_{max}^{ij} \tag{6}$$

The radial displacement d_{rad} can be calculated as the distance between pixel ij and pixel lk

6. Repeat steps 1 through 5 for all pixels to obtain a *Velocity Map* in both the axial and radial directions

The original method proposed by Mosorov et al. [7] was aimed at estimating the axial component of the velocity more accurately as this is the component of velocity that contributes directly to flow rate estimation. Although Mosorov et al. [7] hinted at the possibility of obtaining the direction of the velocity, this was not analyzed in any great detail. Moreover, any difference between the results of the normal image cross correlation and the proposed method was attributed to changes in the flow pattern between plane 1 and 2, an example being a bubble changing its shape, orientation or otherwise transforming itself as it passes through the measurement volume.

But it is not hard to imagine a swirling flow which could also cause pixels to get correlated to their neighbours without the bubble rotating or changing its shape in any way at all. Thus, applying the above described method, a map of the movement of pixels can be obtained for the pipe cross section. Figure 7a shows the direction of the velocity vectors between the two planes of measurement. Figure 7b shows the same data in 3 dimensional form clearly showing the swirling nature of the flow.

Figure 7 only show the direction of flow velocity and not the magnitude in the radial direction. A detailed quantitative analysis follows in the next section.

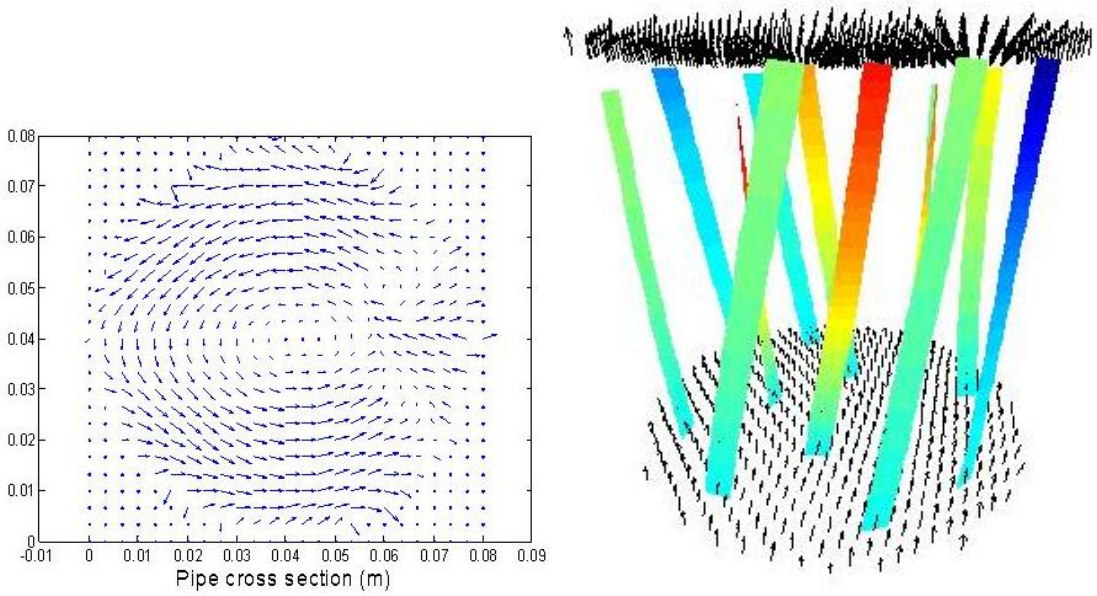

(a) Velocity vectors

(b) Velocity vectors in 3D

Figure 7: *Swirl measurements from impedance cross correlation (SWRi test data)*

4.2 Swirl characterization

The modified image cross correlation technique from the previous section results in a measure of the magnitude and direction of the velocity vector at each pixel in the cross section. Additionally, this information can also be tracked over time. Figure 8a shows the magnitude of the in-plane velocity and 8b shows the deviation (in degrees) of the velocity vector from the vertical direction also called the swirl angle. The swirl angle at a particular pixel ij is defined as

$$SwirlAngle_{ij} = tan^{-1} \frac{|\, Vaxial_{ij} \,|}{|\, Vradial_{ij} \,|} \tag{7}$$

The reason why the two are almost identical is because in simple terms, what causes the deviation of the velocity vector from the vertical direction is the magnitude of the in-plane velocity component. So, the higher the in-plane velocity, the larger the angle of the velocity vector.

For an ideal vertical flow, both these graphs would read 0. So, in essence these two quantities characterize the swirl in the flow. As is evident from figure 7, the information about swirl is multidimensional, and the data needs to be reduced in a way that allows for comparison between different data sets. Swirl angle is a

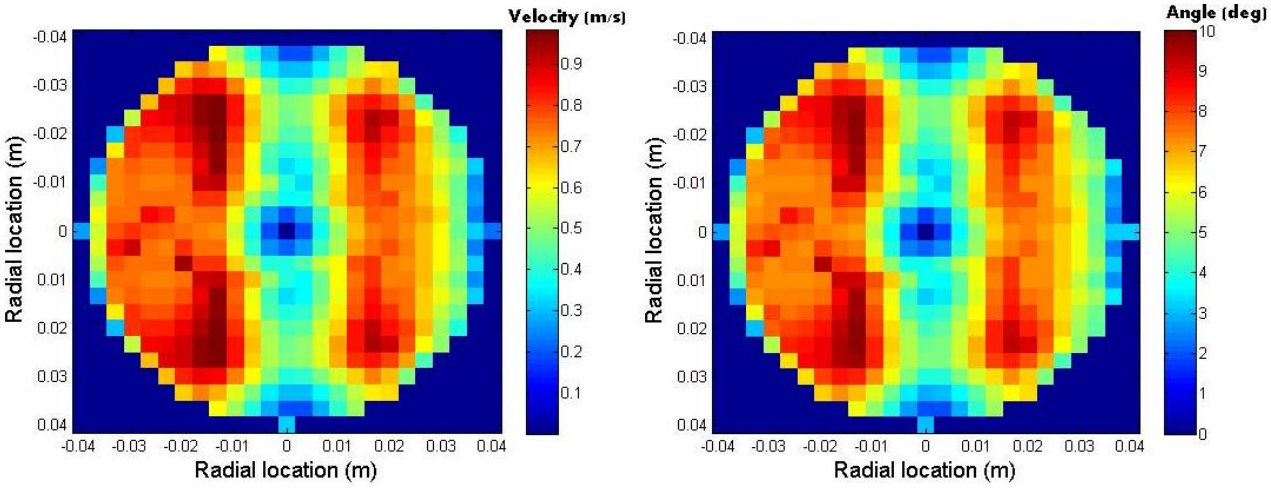

(a) Magnitude of in-plane velocity

(b) Angle of velocity vector with respect to vertical

Figure 8: *Magnitude of in-plane velocity and angle of velocity vector*

metric that is commonly used to quantify swirl. It is both easy to interpret and intuitive. With this particular measurement method, the swirl angle is also very easily calculated as the average of the angle shown in figure 8b. Apart from this, the average angle is an objective metric for two reasons. One is that it will always be a positive number greater than or equal to 0, as is evident from its definition in equation 7. The second is that the higher this number, the larger the deviation from an ideal flow (i.e flow confined only to the vertical direction with no swirl).

Applying this metric on the SWRI test data, figure 9 shows the swirl angle as a function of GVF and gas flow rate at measurement conditions. This data includes variations in flow rates along with the line pressure varying between 10 bar and 100 bar.

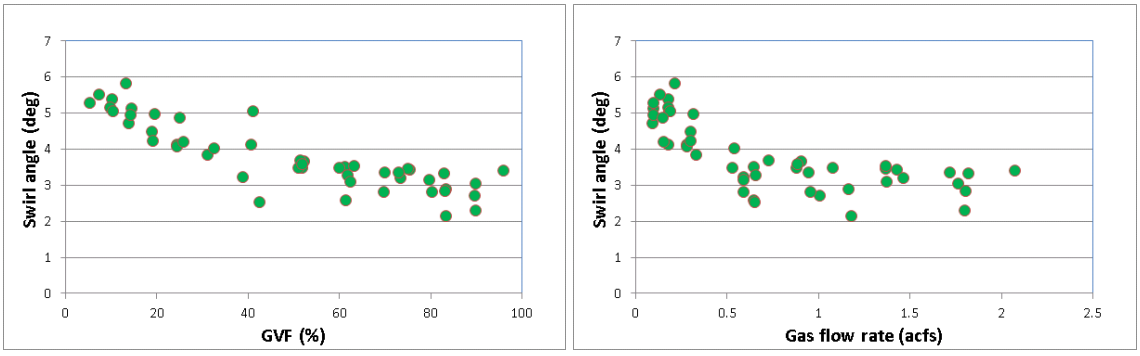

(a) Swirl angle vs GVF

(b) Swirl angle vs Gas flow rate (actual)

Figure 9: *Swirl angle for various flow conditions*

4.3 Error correction based on swirl measurement

Swirling flows are characterized by the presence of rotating velocity components perpendicular to the direction of flow. In other words, there is a velocity component in the pipe cross-sectional plane along with the velocity component along the pipe axis. Such velocity profiles could be a source of error in the flow rate estimation models of different types of sensors. The discharge coefficient of the venturi, for example, is based on a calibration with developed flows confined to the vertical direction. This relationship assumes that the pressure measurements with gauge tapping at the cylinder wall can directly be related to the axial flow since non-swirling flows do not have a pressure gradient in the radial direction. This section is aimed at analyzing the effect of swirling motion on flow estimation, where an analytic model using the phase fraction and velocity information measured from impedance sensors is proposed. This model estimates the correction needed in the differential pressures (dP) to account for swirl.

As has been shown in the preceding sections, there both exist in-plane (cross-sectional) as well as axial velocity components, possibly due to certain upstream conditions such as the blind tee. These give rise to an in-plane pressure profile which needs to be accounted for when interpreting the pressure drop measurements.

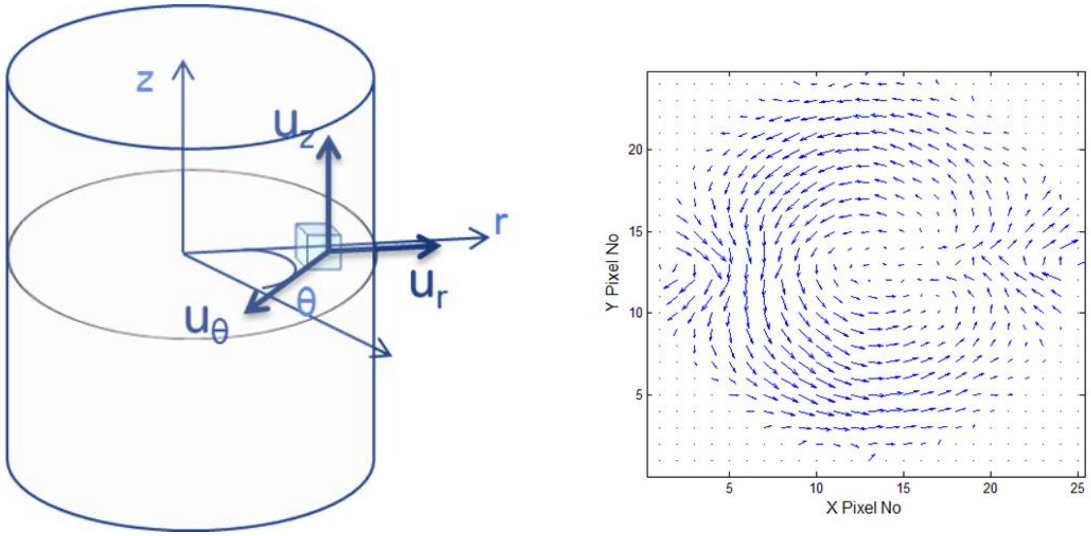

(a) Fluid element schematic

(b) In plane velocity vectors

Figure 10: *In plane velocity profile for a swirling flow*

Consider a spatial fluid element as shown in figure 10a. Starting from the Navies Stokes equation in cylindrical co-ordinates, for an incompressible (density $\rho = constant$), isothermal, inviscid flow and a velocity vector $\overrightarrow{V} = (u_r, u_\theta, u_z)$, in the radial direction we have:

$$\rho\left(\frac{\partial u_r}{\partial t}+u_r\frac{\partial u_r}{\partial r}+\frac{u_\theta}{r}\frac{\partial u_r}{\partial \theta}-\frac{u_\theta^2}{r}+u_z\frac{\partial u_r}{\partial z}\right)=-\frac{\partial P}{\partial r} \tag{8}$$

It is not easy to find an exact solution for equation 8 to find the pressure distribution in the cross section. To make the analysis easier, consider the special case of a steady state, axi-symmetric ($u_r = 0, \frac{\partial}{\partial \theta} = 0$) and developed flow ($\frac{\partial}{\partial z} = 0$), where equation 8 reduces to:

$$\frac{\partial P}{\partial r}=\rho\frac{u_\theta^2}{r} \tag{9}$$

While some of these assumptions may not be valid for the conditions tested, the aim is to obtain an approximate measure of the pressure distribution. Using equation 9, if the local density and in-plane velocities are known, an approximation to the pressure profile in the plane perpendicular to the flow direction can be derived. The local density can be easily obtained using the phase fraction distribution along with the fluid densities. This information is already available to us as a result of the image reconstruction procedure mentioned in section 2.3. The pressure sensors for the differential pressure measurement are flush mounted to the edge of the pipes and essentially capture the local pressure. In case of a non-swirling turbulent flow, this is equal to the mean pressure across the cross-section. For swirling flows, as is evident from equation 9, a radial pressure gradient exists and the pressure at the edges is higher than at the swirl center. The difference between the pressure the centre and that closer to the wall for each pixel experiencing a sample swirling flow is shown in figure 11.

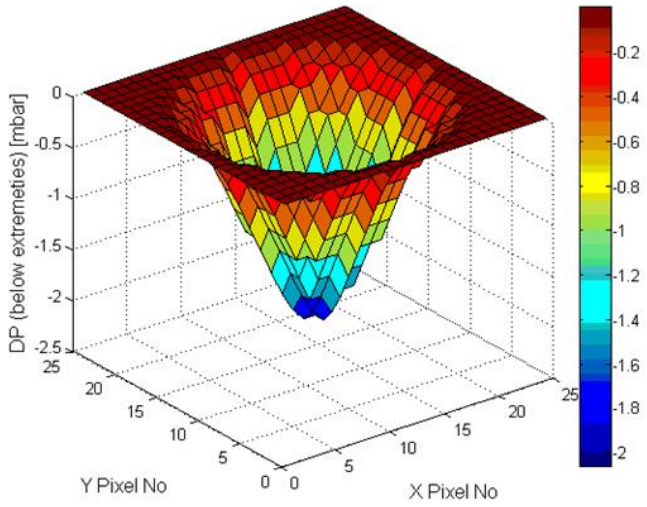

Figure 11: *In-plane pressure distribution for a swirling flow (SWRI test data)*

Using this information, the correction required in the pressure measurement can be computed, at the location that swirl is measured. For the SWRI experiments, using the in-plane pressure profile information in 11, the pressure correction required as a function of GVF is shown in figure 12a. It is seen that the pressure correction required increases with the swirl angle. A higher swirl angle suggests more in-plane velocity contribution to the pressure measured and hence the greater the correction to the dP. The trend with GVF is consistent with the trend of increasing swirl angle with GVF seen in 9a.

To estimate the effect on flow parameters, consider a hypothetical venturi (with beta=0.67) installed at the location of the swirl measurement with dP measurements being made under the flow conditions tested. Assuming that the swirl completely diffuses moving from the upstream of the venturi pressure tapping to its downstream measurement location, the absolute pressure correction shown in figure 12a can be expressed as a percentage of the pressure drop across the venturi. The plot as a function of GVF for the SWRI experimental setup is shown in figure 12b. Since the expression used to determine the pressure distribution is an approximation and not an exact solution, this gives us an order of magnitude for the error in mass flow rate estimation when not accounting for the in-plane pressure gradients.

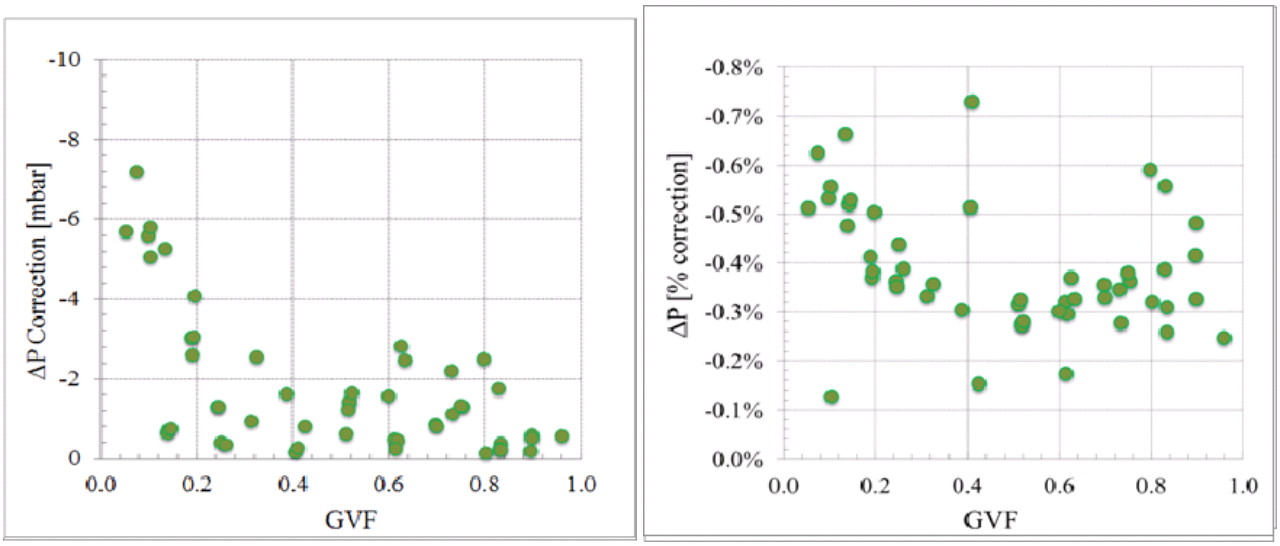

(a) DP correction vs GVF

(b) DP error for a venturi measurement

Figure 12: *Differential pressure correction based on swirl*

5 Conclusions

There are many sources of errors that affect a multiphase flow measurement. The most insidious of these errors are the ones buried in the assumptions either explicitly or implicitly built into the measurement. Flow profile irregularities and asymmetries belong to this category. The problem may be exacerbated if such effects are corrected for using data based calibrations. Such calibrations typically do not capture variations in the flow characteristics with changes in say the flow regime or a fluid property such as the viscosity. Using robust measurements from appropriate sensors and processing methods that can provide invaluable insights about the flow, we have shown in this paper that the flow can be characterized in great detail including not just the distribution of fractions and velocity but also the direction of the flow. The analysis presented in this paper shows that the flow asymmetries and irregularities are an undeniable part of multiphase flow and it would be prudent to acknowledge and account for them in flow rate estimation. While fraction and velocity distribution information can be used in prediction and estimation models such as slip models, the direction information can be used to correct for inaccuracies in sensor measurements such as the venturi differential pressure. Such measurement based corrections are more robust and far more reliable than the empirical corrections that are typically incorporated in flow estimation models to improve their accuracy. Future work will involve analysis of flow profiles for a wider variety of operating conditions and incorporating this information in multiphase flow measurement models to reduce the uncertainty in flow rate estimation.

References

[1] M. Abdulkadir, V. Hernandez-Perez, I. S. Lowndes S. Sharaf, and B. J. Azzopardi. “Experimental investigation of phase distributions of two-phase air-silicone oil flow in a vertical pipe”. In: *World Academy of Science, Engineering and Technology* 37 (Jan. 2010), p. 52.

[2] S. Al-Hinai. “Non-invasive velocity and volume fraction profile measurement in multiphase flows”. Doctoral thesis. University of Huddersfield., 2010.

[3] J Gibson and M Reader-Harris. “Swirling flow through venturi tubes of convergent angle 10.5Âř and 21Âř”. In: *ASME Joint U.S. - European Fluids Engineering Summer Meeting*. 2006.

[4] A Gupta and R Kumar. “Three-dimensional turbulent swirling flow in a cylinder: Experiments and computations”. In: *Internation journal of heat and fluid flow* 28 (2007), pp. 249–261.

[5] S. Mahalingam, A. Banerjee, W. Basu, and H. K. Pillai. “Electrical network analysis of a multiphase system”. US Patent 8121804. General Electric Company. 2012.

[6] S. Mahalingam, M. K. Koyithitta Meethal, A. Banerjee, W. Basu, and H.K. Pillai. “Electrical network representation of a distributed system”. US Patent 8264246. General Electric Company. 2012.

[7] V. Mosorov, D. Sankowski1, L. Mazurkiewicz, and T. Dyakowski1. “The "best-correlated pixels" method for solid mass flow measurements using electrical capacitance tomography”. In: *Measurement Science and Technology* 13 (2002), pp. 1810–1814.

[8] A. Ohnuki and H. Akimoto. “Experimental study on transition of flow pattern and phase distribution in upward air water two-phase flow along a large vertical pipe”. In: *International journal of multiphase flow* 26 (Mar. 2000), pp. 367–386.

[9] A Rammohan, A Dixit, V Natrajan, and M Kumar. “Detailed review of existing empirical and analytical estimation models for multiphase flow”. In: *30 North Sea Flow Measurement Workshop*. 2012.

[10] T. K. Thiyagarajan, P. Satyamurthy, N. S. Dixit, A. Garg N. Venkatramani, and N. R. Kanvinde. “Void fraction profile measurements in two-phase mercury-nitrogen flows using gamma-ray attenuation method”. In: *Experimental thermal and fluid science* 10 (3 1995), pp. 347–354.